

## Parasitic stage of *Ostertagia ostertagi*: A mathematical model for the livestock production region of Argentina



M.A.E. Chaparro<sup>a,b,\*</sup>, G.A. Canziani<sup>b</sup>, C.A. Fiel<sup>c</sup>

<sup>a</sup> CONICET, Rivadavia 1917, C1033AAJ Ciudad Autónoma de Buenos Aires, Argentina

<sup>b</sup> Instituto Multidisciplinario sobre Ecosistemas y Desarrollo Sustentable, Facultad de Ciencias Exactas, Universidad Nacional del Centro de la Provincia de Buenos Aires (UNCPBA), Pinto 399, B7000GHG Tandil, Argentina

<sup>c</sup> Dpto. de Sanidad Animal y Medicina Preventiva (SAMP), Facultad de Ciencias Veterinarias, UNCPBA, Pinto 399, B7000GHG Tandil, Argentina

### ARTICLE INFO

#### Article history:

Received 29 August 2012

Received in revised form 30 April 2013

Accepted 2 June 2013

Available online 3 July 2013

#### Keywords:

Fuzzy rule based systems

Gastrointestinal nematodes

Inhibition–disinhibition

Population dynamic

### ABSTRACT

The model here presented describes the dynamics of adult *Ostertagia ostertagi* parasites in cattle in the field. The model also describes the population of infecting L3 larvae subject to the conditioning process while in the pasture as well as the inhibition–disinhibition process in ingested L4 larvae. The model has two modules: one for the conditioning process and the other for the parasitic stage. The first module determines the proportion of ingested L3 larvae that will go through an arrested stage of development, or hypobiosis, and for how long depending on the weather conditions and the length of the period of exposure in the pasture. The second one describes the adult population dynamics as disinhibiting larvae and recently ingested larvae accumulate in the animal. The model has a discrete daily step and is parameterized using fuzzy inference systems of the Mamdani type (FM). Given that the inhibition–disinhibition process is not yet fully understood, a series of perturbations on the different input variables were performed with the purpose of analysing the model's behavior. Simulations show that the adult population exhibits two maximal peaks of infection in the hosts in December–January (Summer) and April–May (Autumn). These high values are a consequence of hypobiotic larvae resuming their development at those times.

© 2013 Elsevier B.V. All rights reserved.

### 1. Introduction

*Ostertagia ostertagi* is the predominant cattle parasite in the temperate region of Argentina. The most important effects in the cattle caused by deficient parasite control, or simple lack of it, are losses ranging from calf mortality to significant reductions in animal weight gain as well as reductions in milk production. Mortality is rare, but it usually occurs as a consequence of bodily decay, nutrient loss, diarrhea and dehydration. It affects less than 3% of the post-weaning calves during their first winter. A reduction in weight gain was estimated to affect some 18% of animals feeding in natural pastures and 25% of those feeding in pens. This reduction is due to the lack of appetite and modifications on the digestion process. According to tests performed in an experimental agricultural station (INTA-EEA Anguil, Argentina) the largest losses occur during the first autumn–winter grazing. Animals suffer losses ranging from 18 to 44 kg in calves and 15 to 23 kg to steers. It is worth noting that this gastrointestinal nematodosis produces a delay on the sexual development of steers. An essay realized by INTA-EEA

Anguil with Aberdeen Angus cattle yielded that steers with parasites reached the sexual maturity at 18 months of age while animals without parasites reached it at 15 months (Suárez, 2005). From an economic perspective, estimated costs in 1998 added up to some 22 million dollars in annual losses due to cattle mortality, and 170 million dollars caused by subclinic problems.

The life cycle of the nematode *O. ostertagi* is direct without intermediate host. It has two stages, one called “free living stage” (Egg–L1–L2–Infective larva (L3)) and the other “parasitic stage” (L3–L4–L5–Adult). The free-living stage occurs on the ground, first within the dung-pat and later on the grass. Larvae in the L1 and L2 stages feed on fungi and bacteria. The infective larva (L3) is ensheathed and does not feed. Following its ingestion by the bovine, L3 larvae undergo a process of exsheathment in the rumen before the fourth parasitic stage begins (L4). Then L4 larvae develop into the adult stage. The prepatent period is usually about three weeks, however the parasite can arrest its development thus extending the cycle for several months. This phenomenon is called hypobiosis, inhibited development, or arrested development. For *O. ostertagi* this phenomenon occurs in the early parasitic stage.

Previous studies (Fernández et al., 1999; Lützelshwab et al., 2005) suggest that the inhibition process in *O. ostertagi* depends on the weather conditions to which the infective L3 larvae are exposed

\* Corresponding author. Tel.: +54 2293 439688; fax: +54 2293 439688.

E-mail address: [chaparromauro76@gmail.com](mailto:chaparromauro76@gmail.com) (M.A.E. Chaparro).

on pasture, and the length of time that *L3* larvae spend on pasture. In temperate regions of the Northern hemisphere, hypobiosis occurs in autumn and early winter (Couvillion et al., 1996), but in the Southern hemisphere (particularly in Argentina) there is evidence that this phenomenon occurs in spring and early summer (Fiel et al., 1988; Suárez, 1990; Fernández et al., 1992, 1999; Descarga et al., 1994; Lützelshwab et al., 2005).

In Argentina, the disinhibition process is not fully understood, but based on results reported by Fiel et al. (2009) it is possible to infer that it occurs in two consecutive “disinhibition waves”, the first extending from November to early January and the second from mid-February to the end of April.

It is worth noting that the hypobiotic larvae are metabolically depressed and, therefore, they are less susceptible to anthelmintics such as Levamisole, Benzimidazoles, Ivermectin, Doramectin or Moxidectin. Hence for an efficient sanitary control, it becomes both important and necessary to understand the pattern of infection on pasture and the effects post-grassing.

A model build by Ward (2006a,b) was based on dynamic systems theory. It is worth noticing that this model is not for just *Ostertagia*, but for all gastrointestinal roundworms in cattle. Ward’s model takes into account some aspects of the life cycle of parasites that we do not consider adequate because of the above-mentioned evidence. Ward considered that temperature is the only variable that affects the inhibition–disinhibition process, but it is clear that in this region more variables are involved in this process (Lützelshwab et al., 2005). On the other hand, the disinhibition process in Ward’s model was considered to be constant, 130 days post-ingestion, without taking into account the time of the year when the larvae are ingested. As mentioned earlier, Fiel et al. (2009) observed two distinct waves of disinhibition (early January and end of February) under normal conditions in the Humid Pampas.

There are many experimental studies in Argentina that allow proposing a descriptive statistical analysis about this problem but there are no mathematical models about the dynamics of *O. ostertagi* that are able to mimic this particular dynamics. In recent years we proposed a model to estimate the time of development from egg to infective larva (Chaparro and Canziani, 2010) and a model of the free living stages (Chaparro and Canziani, 2010; Chaparro et al., 2011). Here we propose a mathematical model for the parasitic stage of *O. ostertagi*, including hypobiosis, adapted to the environmental conditions in the Pampas region of Argentina, which extends roughly from latitudes 30° S to 40° S. The model describes the population dynamics of infective larvae (*L3*), hypobiotic larvae (*L4h*) and parasite adults (*A*). It is worth noting that with the concatenation of this model to the above-mentioned ones the life cycle of *O. ostertagi* is thus completed.

## 2. Materials and methods

### 2.1. Model description

As mentioned before, the model describes the population dynamics of *L3* larvae in the pasture, the hypobiotic larvae (*L4h*) and adults (*A*) with a daily step. It takes into account the weather conditions and the infection levels in pasture. Infection levels are measured as number of larvae per kilogram of dried grass.

There is sufficient evidence that the processes of inhibition and disinhibition are related to the weather conditions to which the infective larvae were exposed before being ingested by the animal (Fernández et al., 1999; Lützelshwab et al., 2005; Langrová et al., 2008; Fiel et al., 2009). Therefore, the model is composed of two modules. The first module describes the dynamics of the *L3* larval population in the pasture waiting to be ingested. The second module describes the dynamics of the *L4–L4h* and adult populations inside the animal. The conceptual model is shown in Fig. 1.

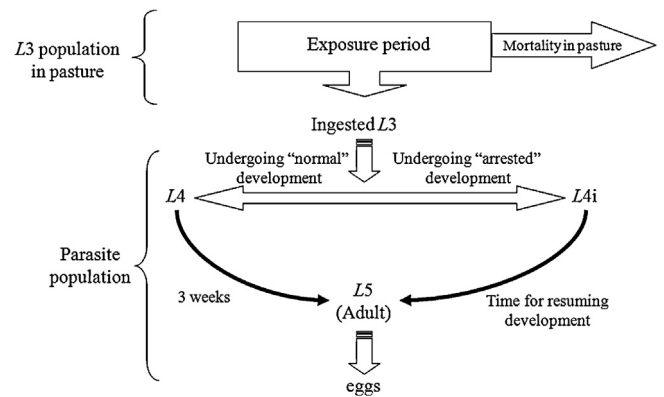


Fig. 1. Diagram of the model.

#### 2.1.1. The model for the infective larvae population in the pasture

The dynamics of the population in the pasture is regulated by weather conditions, more precisely by rainfall and temperature (Chaparro et al., 2011; Fiel et al., 2012). From the view point of the model, this dynamics can be summarized in two processes:

1. Contribution through migration of *L3* from dung to pasture.
2. Reduction of the larval population caused by:
  - a. ingestion of larvae by cattle, and
  - b. natural mortality.

Let  $L3_p(k)$  be the total number of *L3* in pasture on julian day “*k*”. The population dynamics is described by:

$$L3_p(k) = C_k(0) + \sum_{i=1}^{k-1} C_i(k-i), \quad (2.1.1.1)$$

where  $C_j(a)$  is the number of members of the *j*th *L3* cohort, that is, those larvae migrating to pasture on julian day *j*, with cohort age *a*.

Each cohort  $C_m(\cdot)$ , can only be affected by removal of *L3* larvae either by mortality or by ingestion. Then, the amount of *L3* larvae in each cohort *m* is described by:

$$C_m(a+1) = (1 - \mu_p(m, a))C_m(a) - p(m, a)I(a+m), \quad (2.1.1.2)$$

where  $\mu_p(m, a)$  and  $p(m, a)$  are the mortality in pasture and the probability of a larva of the cohort  $C_m(a)$  being ingested, respectively;  $I(a+m)$  is the total amount of larvae ingested on *a+m* julian day by cattle. A constant daily mortality rate on pasture of 0.003 was used, following Leathwick et al. (1992).

Assuming a uniform distribution of *L3* larvae in pasture, the value  $p(m, a)$  is calculated by:

$$p(m, a) = \frac{C_m(a)}{L3_p(a+m)} \quad (2.1.1.3)$$

This description of individuals that compose the *L3* population on pasture allows keeping track of:

- the total number of larvae belonging to the *i*th cohort that were ingested, and
- the length of time and the environmental conditions to which the larvae were exposed.

This information is important for calculating the proportion of *L3* that will go through the inhibition stage.

2.1.2. Model for calculating the amount of adult parasites in the host

We assume that the length of time a L3 larva spends on pasture does not directly affect the parasite population but does modify its dynamics when inside the host.

Let  $I(k)$  be the amount of larvae ingested on julian day  $k$ . This set is composed by larvae belonging to different cohorts. Therefore, if  $I(j,k)$  is the set of ingested larvae from the  $C_j(k)$  cohort, then we can calculate  $I(j,k)$  by:

$$I(j, k) = p(j, k)I(k + j) = \frac{C_j(k)}{L3P(k + j)}I(k + j), \tag{2.1.2.1}$$

Let  $p_{Hyp}(j,k)$  be the proportion of hypobiotic larvae of the  $j$ th cohort aged  $k$ , then the amount of hypobiotic larvae  $L4_H(k)$  on day  $k$  is:

$$L4_H(k) = \sum_{j=1}^k p_{Hyp}(j, k)I(j, k). \tag{2.1.2.2}$$

Then the non-hypobiotic larvae  $L4(k)$ , those which go through a normal development, are:

$$L4(k) = I(k) - L4_H(k). \tag{2.1.2.3}$$

Finally, the total amount of adults within the host on julian day  $t$  is the sum of:

- the number of adults that survive from the previous of day, given by  $(1 - \mu(t))A(t - 1)$ ;
- the number of L3 larvae ingested three weeks before (prepatence period) which do not inhibit their development, given by  $L4(t - 21)$ ; and
- the number of hypobiotic larvae that resume their development, given by

$$\left( \sum_k L4_H(k + DHyp(k)) \quad \forall k/k + DHyp(k) = t \right)$$

Thus, the equation that describes the adult parasite population is:

$$A(t) = (1 - \mu(t))A(t - 1) + L4(t - 21) + \sum_{\forall k/k + DHyp(k)=t} L4_H(k + DHyp(k)). \tag{2.1.2.4}$$

where  $DHyp(k)$  is the disinhibition time.

**Table 1**  
Membership functions of the fuzzy inference system (FIS) used in calculating the proportion of hypobiotic larvae.

| Variable lingüística           | Name of membership function | Type         | Parameters values |      |      |       |
|--------------------------------|-----------------------------|--------------|-------------------|------|------|-------|
|                                |                             |              | a                 | b    | c    | D     |
| Time of exposure (input)       | T-m                         | Z(x;a,b)     | 3                 | 4    |      |       |
|                                | F1                          | Tri(x;a,b,c) | 3                 | 6    | 7    |       |
|                                | F2                          | Tri(x;a,b,c) | 6.5               | 8    | 10   |       |
|                                | F3                          | Tri(x;a,b,c) | 9.9               | 12   | 14   |       |
|                                | T-M                         | S(x;a,b)     | 13.5              | 16   |      |       |
| Daily mean temperature (input) | D2                          | Z(x;a,b)     | 9.1               | 12.5 |      |       |
|                                | D4                          | Tri(x;a,b)   | 9.1               | 12.5 | 15.5 |       |
|                                | D6                          | Tri(x;a,b)   | 12.5              | 16   | 19.8 |       |
|                                | D8                          | S(x;a,b)     | 16.5              | 19.8 |      |       |
| Daily photoperiod (input)      | Fot1                        | Z(x;a,b)     |                   |      |      |       |
|                                | Fot2                        | Trap(x;a,b)  | 11.1              | 13   | 14.4 | 14.55 |
|                                | Fot3                        | S(x;a,b)     | 14                | 14.7 |      |       |
| Hypobiotic larvae (output)     | Low                         | Tri(x;a,b)   | 0                 | 6    | 12   |       |
|                                | Moderate                    | Tri(x;a,b)   | 10                | 25   | 60   |       |
|                                | High                        | Tri(x;a,b)   | 50                | 75   | 90   |       |

**Table 2**  
Base of rules for the fuzzy inference system used *i* calculating the proportion of hypobiotic larvae ( $L4_H$ ).

| Time | Temperature | Photoperiod | Hypobiotic |
|------|-------------|-------------|------------|
| 1    | 2           | 2           | 2          |
| 2    | 2           | 2           | 3          |
| 3    | 2           | 2           | 3          |
| 4    | 2           | 2           | 2          |
| 1    | 3           | 2           | 2          |
| 2    | 3           | 2           | 3          |
| 3    | 3           | 2           | 3          |
| 4    | 3           | 2           | 1          |
| 1    | 4           | 2           | 3          |
| 2    | 4           | 2           | 2          |
| 3    | 4           | 2           | 1          |



2.1.3. Model for calculating the proportion of hypobiotic larvae ( $L4_H$ )

We construct a fuzzy Mamdani type inference system (FIS) (Klir and Yuan, 1995; Nguyen and Walker, 1997) for calculating the proportion of ingested larvae that arrest their development in response to environmental conditions.

The input variables are:

- Length of time of exposure of the L3 cohort to environmental conditions (days).
- Daily mean temperature (°C).
- Photoperiod in the study zone (hours).

These input variables were selected and their membership functions were constructed based on the information reported in studies carried out in the Humid Pampas region by Fernández et al. (1999), Lützel Schwab et al. (2005), and Fiel et al. (2009). The complete list of membership functions and the base rules of the system are summarized in Tables 1 and 2, respectively. The surface output for different exposure times are shown in Fig. 2.

2.1.3.1. Time of exposure. The period of inhibitory activity in the Humid Pampas region is reported as starting at the end of August and lasting until the end of December, which corresponds to Spring–early Summer. Past the end of December, regardless of the length of exposure, the capacity for developmental arrest seems to be lost (Lützel Schwab et al., 2005).

Lützel Schwab et al. (2005) report a minimum time of exposure to environmental conditions as well as the weather conditions required for *O. ostertagia* larvae to arrest their development within the host. During September–October, the length of time

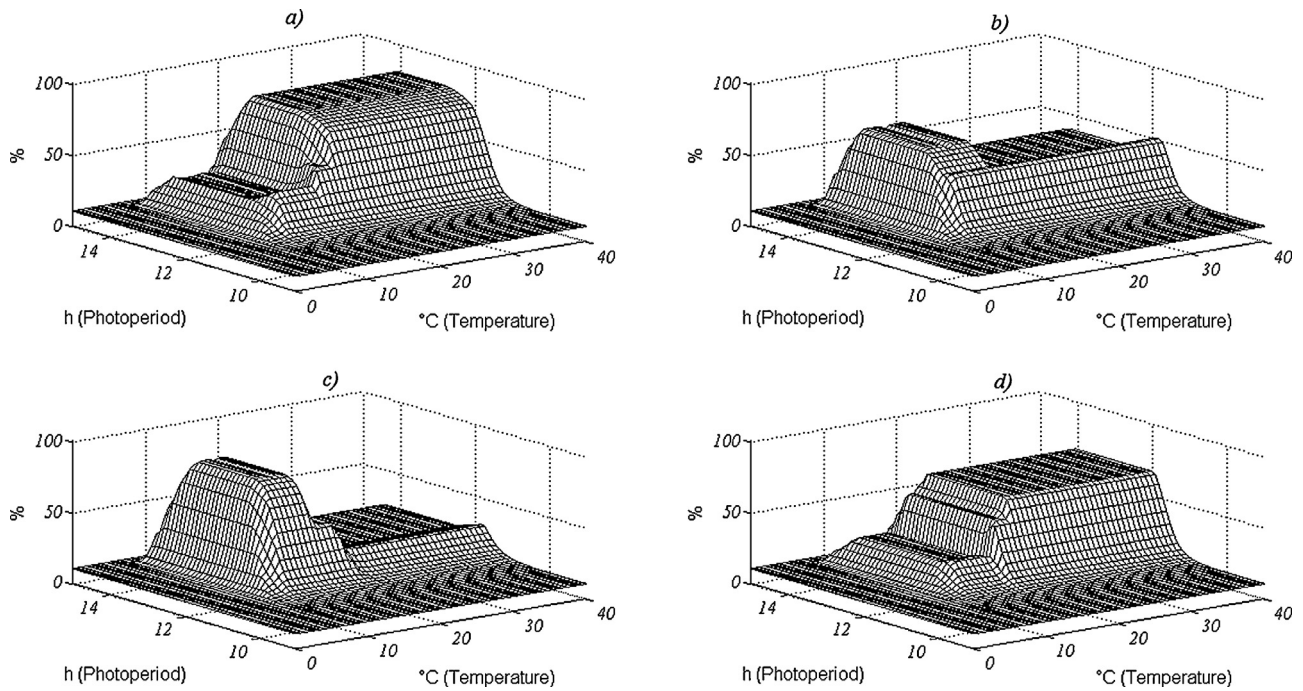


**Fig. 2.** Output of the fuzzy inference system (proportion of ingested larvae that arrest their development) for (a) 3, (b) 5, (c) 7 and (d) 12 weeks of exposure to environmental conditions.

necessary to obtain some 50% of inhibited larvae under field conditions was three weeks. During November, about 60% of parasites were inhibited after only one week. In December, the time of exposure was less than one week, but the activity stopped at the end of the month. Beyond this period, the proportion of hypobiotic larvae was assumed to be null. Thus, twenty weeks are the maximum exposure time considered in this model. Based on these studies, the use of five membership functions seems the most appropriate for representing the twenty-week period (end of August–end of December). The type of functions chosen and their parameters are summarized in Table 1.

**2.1.3.2. Daily mean temperature.** After analysis of the data set of daily mean temperatures from 1990 to 2008, we chose to construct four membership functions. Each function has its maximum value of membership corresponding to the deciles 2nd, 4th, 6th, 8th of the data set, respectively. The type of functions and their parameters are summarized in Table 1.

**2.1.3.3. Daily photoperiod.** During the essays carried out and reported by Lützelshwab et al. (2005), inhibition of more than 50% of ingested larvae was found to occur with a photoperiod ranging between 13 and 14 h. The highest proportion of  $L_{4H}$  (average 75%) in the hosts was found with a 14 h 43 min photoperiod. Therefore a photoperiod function was formulated as:

$$\text{Phot}(t) = \frac{24}{\pi} \ar \cos \left( -\text{tg}(\text{lat}) \text{tg} \left( 0.4093 \text{sen} \left( \frac{2\pi t}{365} - 1.405 \right) \right) \right), \quad (2.1.3.3.1)$$

where  $t$  is the julian day and  $\text{lat}$  is the latitude of the study zone.

For example, the photoperiod for Tandil ( $37^{\circ}19'08''$  S) varies from 9 h 35' (21st June) to 14 h 48' (21st December).

From the view point of the inhibition phenomena, the ideal photoperiod is between 12 h 11 min a 14 h 55 min. Fiel et al. (2009) report that for shorter or longer photoperiods the larvae do not seem to be able to go through hypobiosis. It is worth noting that Spring and Autumn have equal photoperiod amplitudes. Despite

this fact, in Autumn the inhibition activity is null. We believe that the differences are due to daily temperature and the fact that in Spring the photoperiod is increasing while in Autumn the photoperiod is decreasing. Three membership functions were used, one corresponding to the Summer photoperiod, one for the Winter photoperiod, and one for the Spring–Autumn photoperiod. The type of function and their parameters are summarized in Table 1.

**2.1.3.4. The proportion of  $L_3$  that will become hypobiotic larvae ( $L_{4H}$ ).** The membership functions for the daily proportion of ingested  $L_3$  larvae that will become hypobiotic larvae were build based on field essay data from Lützelshwab et al. (2005), Fiel et al. (2012), and experimental laboratory data from Fernández et al. (1999), as well as expert empiric knowledge three triangular membership functions were used to characterize the observed proportions. The function parameters are summarized in Table 1.

#### 2.1.4. Disinhibition

The function that models the photoperiod has four critical points related to solstices and equinoxes (21st December, 21st March, 21st June and 21st September). The photoperiod function attains the maximum and minimum values in December and June, respectively, while the inflexion points correspond to equinoxes in March and September. The rate of increase (derivative) of the photoperiod function is positive from June 21 to December 21, but increases from June 21 until reaching its maximum on September 21 and then decreases until December 21. The hypothesis is that this change in the velocity of function's growth rate (second derivative) determines when the  $L_3$  ingested by the host resume their development. The  $L_3$  larvae ingested before the Spring equinox seem to resume their development before January. This period has at most 65 days. The larvae ingested after the Spring equinox seem to resume their development past March. Therefore this period lasts a maximum of 5 months (Fig. 3).

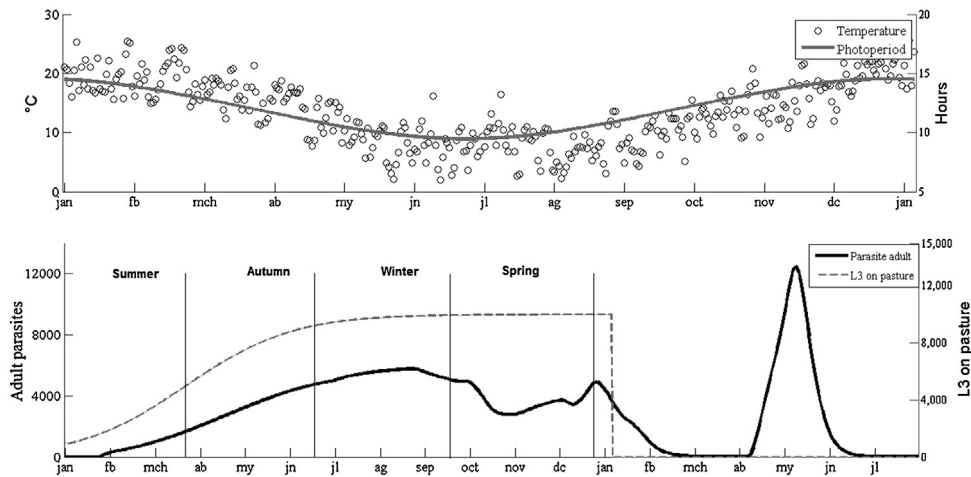


**Fig. 3.** (a) Photoperiod (—) and temperature (○) series for Tandil from 2006 to 2008. (b) The total of L3 on pasture (···) and the result of the simulation (—) performed using the data set of environmental conditions corresponding to Tandil over the years 2006–2008, a constant availability of L3 on pasture of 1000 L3 day<sup>-1</sup> and the daily ingestion rate 0.05 (reference series, RS).

So the disinhibition time, in days, is modeled as:

$$DihT(t) = \begin{cases} 240 - \frac{t}{2} & \text{if } Phot(180) \leq Phot(t) \leq Phot(265) \\ 270 - \frac{t}{2} & \text{if } Phot(t) \geq Phot(265) \\ 0 & \text{if otherwise} \end{cases} \quad (2.1.4.1)$$

## 2.2. Model's response analysis

Perturbations in the input data series (input variables) such as photoperiod, temperature, and seasonal L3 availability in pasture were performed with the purpose of analyzing the effect of each input variables on the model output.

The simulations were performed using one data set of environmental conditions corresponding to Tandil, province of Buenos Aires, over the years 2006–2008.

A simulation was performed using the following input:

- A constant availability of L3 in pasture of 1000 ind.day<sup>-1</sup> (each day, 1000 L3 individuals migrate to pasture).
- Daily ingestion rate 0.05 (5% of L3 larvae in pasture ingested by day).
- Temperature corresponding to Tandil, 2006–2008.
- Latitude: 37° 19' 59" S.
- The animals are fed in the same paddock during one year.

The result of this simulation is being called “reference series” (RS) (Fig. 3).

The numerical experiments correspond to simulations in which one of the input variables was disturbed while the others remained fixed. The Hilbert projective pseudometric was used in order to quantify the effect of perturbations (Caswell, 2001). This metric measures the distance between two nonnegative vectors in a way that depends only on their proportional composition, independent of their absolute size. The metric is defined by:

$$d(x, y) = \log \left( \frac{\max_i \left( \frac{x_i}{y_i} \right)}{\min_i \left( \frac{x_i}{y_i} \right)} \right) = \max_{i,j} \log \left( \frac{x_i y_j}{y_i x_j} \right)$$

where  $x_i$  and  $y_i$  are the elements of vectors  $x$  and  $y$ , respectively.

Therefore, it is possible to classify each experimental series through the effect that the disturbance produced in the output of the model as compared to RS, the reference series.

### 2.2.1. Disturbance in temperature data

The temperature data series corresponding to Tandil over the period 2006–2008 ( $\bar{X} = 14^\circ\text{C}$ ;  $sd = 5.4^\circ\text{C}$ ) was used to analyze the response of the model. The temperature series was disturbed by adding and subtracting 2.5 °C and 5 °C to every entry. Therefore, four new temperature series with the same standard deviation ( $sd$ ) were obtained. The outputs of these simulations were called  $T_{-5^\circ\text{C}}$ ,  $T_{+2.5^\circ\text{C}}$ ,  $T_{+5^\circ\text{C}}$ , respectively.

### 2.2.2. Disturbance in photoperiod

Disturbances in the photoperiod were introduced by changing the latitude in Eq. (2.1.3.3.1). This parameter change allows mimicking different geographical areas because there is a functional relationship between latitudinal coordinates and the corresponding photoperiod. The latitudes selected correspond to different grazing areas of Argentina: Carmen de Patagones, province of Buenos Aires (40° 48' 09" S); Junín, province of Buenos Aires (34° 35' 38" S); Mercedes, province of Corrientes (29° 11' 05" S). The outputs of these simulations were called  $F_{40^\circ}$ ,  $F_{35^\circ}$ ,  $F_{30^\circ}$ , respectively.

### 2.2.3. Disturbance in the seasonal availability of L3 larvae in pasture

The availability of L3 in pasture is clearly seasonal; in particular it is related to the seasonality of rainfall (Chaparro et al., 2011). The input series for the simulations were generated by the following function:

$$P_k(i) = \begin{cases} 1000 & \text{if } i \in [k, k + 90] \\ 0 & \text{otherwise} \end{cases}$$

This function represents daily amount of L3 that migrate to pasture from julian day  $k$  until  $k + 90$ . For example, if  $k = 0$  the function represents Summer.

The outputs of these simulations we called Summer, Autumn, Winter and Spring, respectively. It is worth noting that these simulations represent very unrealistic situations, but from a computational experimental viewpoint is a good way for investigating the particular effect of each season-population on the disease dynamics. The results of these simulations tell in which way the

**Table 3**  
Hilbert distance from the reference series (RS) output to the output of simulations using perturbation series.

| Distance of Hilbert to Rs | Temperature              |                            |                           |                         |
|---------------------------|--------------------------|----------------------------|---------------------------|-------------------------|
|                           | $T_{-5^{\circ}\text{C}}$ | $T_{-2.5^{\circ}\text{C}}$ | $T_{2.5^{\circ}\text{C}}$ | $T_{5^{\circ}\text{C}}$ |
|                           | 1.612                    | 0.777                      | 0.323                     | 1.117                   |
| Distance of Hilbert to Rs | Photoperiod              |                            |                           |                         |
|                           | $F_{30}$                 | $F_{35}$                   | $F_{40}$                  |                         |
|                           | 0.311                    | 0.121                      | 1.023                     |                         |

larvae produced in just one season contribute to maintaining the infection.

### 3. Results and discussion

#### 3.1. Response of the model to perturbations in input variables

##### 3.1.1. Disturbance in temperature data

The values of the Hilbert distance of each output to RS showed that the series  $T_{-5^{\circ}\text{C}}$  was the one exhibiting the largest difference (Table 3). It is worth noticing that when the mean temperature decreased in the series perturbation the effect was larger than when the temperature increased.

For each simulation, the difference between disturbed vs. reference series was plotted into a graph (Fig. 4). This allowed analyzing the magnitude and the timing of the disturbance's effect relative to the reference series. Clearly, the perturbation on the temperature series modified the availability of L3 on pasture and parasite adult population (Fig. 4). A positive difference for the  $T_{-2.5^{\circ}\text{C}}$  and  $T_{-5^{\circ}\text{C}}$  series was observed from December onwards, i.e. the adult population of the RS output was higher than those of  $T_{-2.5^{\circ}\text{C}}$  and  $T_{-5^{\circ}\text{C}}$  for the previous period. This results from the fact that the populations of  $T_{-2.5^{\circ}\text{C}}$  and  $T_{-5^{\circ}\text{C}}$  follow "normally" their development, without arresting their development, and quickly join the adult population.

On the other hand, for higher temperatures a proportion of the ingested L3 of the RS output arrested their development from September to December, therefore the adult population decreases over this period. The difference is positive until April of next year for  $T_{2.5^{\circ}\text{C}}$  and  $T_{5^{\circ}\text{C}}$ , where the second disinhibition "wave" is observed. The dynamics observed in both outputs indicate that the inhibition

levels from October to December are higher for the disturbed series than for the RS series.

Therefore, from the results of these simulations we can conclude that the proportion of hypobiotic larvae decreases when the average temperature decreases and increases when it increases (Fig. 4).

##### 3.1.2. Disturbance on photoperiod

The value of the distance to the RS series showed that the  $F_{40^{\circ}}$  (South of Tandil) is the largest, therefore the effects are more important. The other perturbation series, representing Northern latitudes, do not show important differences (Table 3).

Over the September–November period, the differences between reference series (RS) populations and the populations of adult parasites corresponding to lower latitude input ( $F_{30^{\circ}}$ – $F_{35^{\circ}}$ ) were minor. These differences continued until April and then, from this month onwards, the second wave occurred and the lower latitude series exceeded the RS series until the end of the simulations. For the higher latitude series ( $F_{40^{\circ}}$ ), the behavior was inverted relative to the previous series. The adult population of this simulation was slightly smaller than that of the RS series until April, when the second wave took place. It is worth noting that all series (lower and higher latitude) have two waves of disinhibition but, for the first two the second wave is more important while for the third one the first is higher. The majority of ingested L3 larvae at higher latitude arrested their development before October, while at lower latitudes was after October. The results of all simulations are shown in Fig. 5.

##### 3.1.3. Disturbance on the seasonal availability of L3 larvae in pasture

**3.1.3.1. Summer and autumn.** The L3 larvae ingested during Summer and Autumn showed a "normal" development without any  $L4_H$  observed. The maximum abundance of adult parasites was reached in mid-April (those ingested in Summer) and mid-July (those ingested in Autumn), after what the populations decreased steadily until total disappearance by the end of August and December, respectively. The maximum value reached by the Autumn output is higher than of the Summer output, because the survival of L3 larvae in pasture is lower in Summer than in Autumn. The output of the simulations is shown in Fig. 6.

**3.1.3.2. Winter.** The population ingested in Winter showed a behavior quite different from that of the other seasons. Hypobiotic larvae were observed from August till October (Fig. 6). The maximum value of the adult population was reached in October.

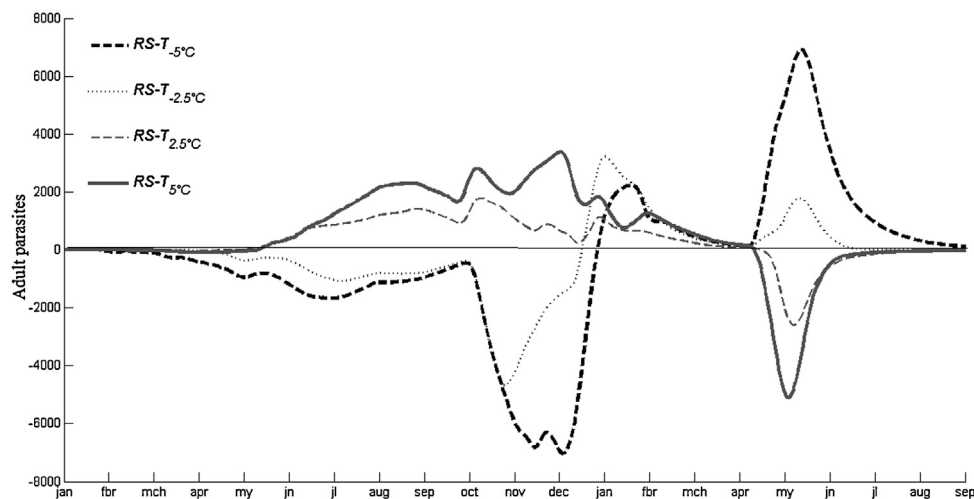


**Fig. 4.** The effects of temperature in the adult parasites population. Each  $RS-T_{\#\#}$  curve corresponds to the difference in the amount of adult parasites between the reference (RS) and the disturbed temperature series. A positive value means that the amount of parasites obtained from RS is higher than that obtained from  $T_{\#\#}$ .

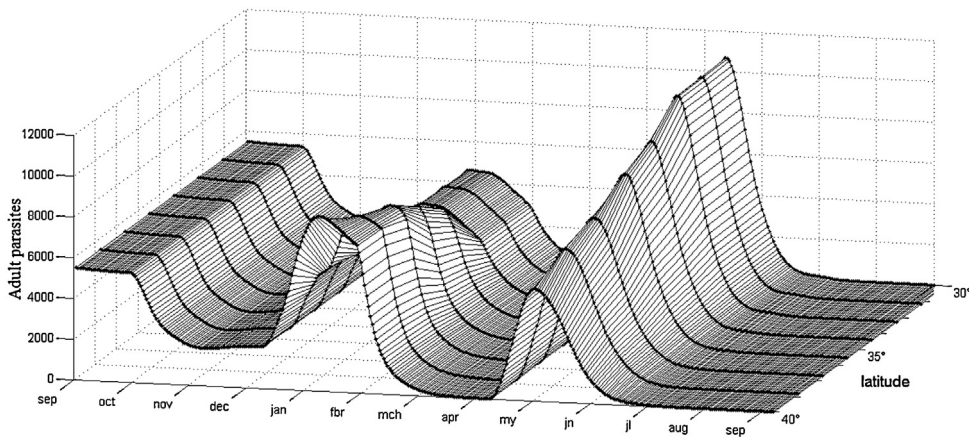


Fig. 5. Results of simulations of the dynamics at different latitudes obtained by changing the latitude in the photoperiod function (2.1.3.3.1).

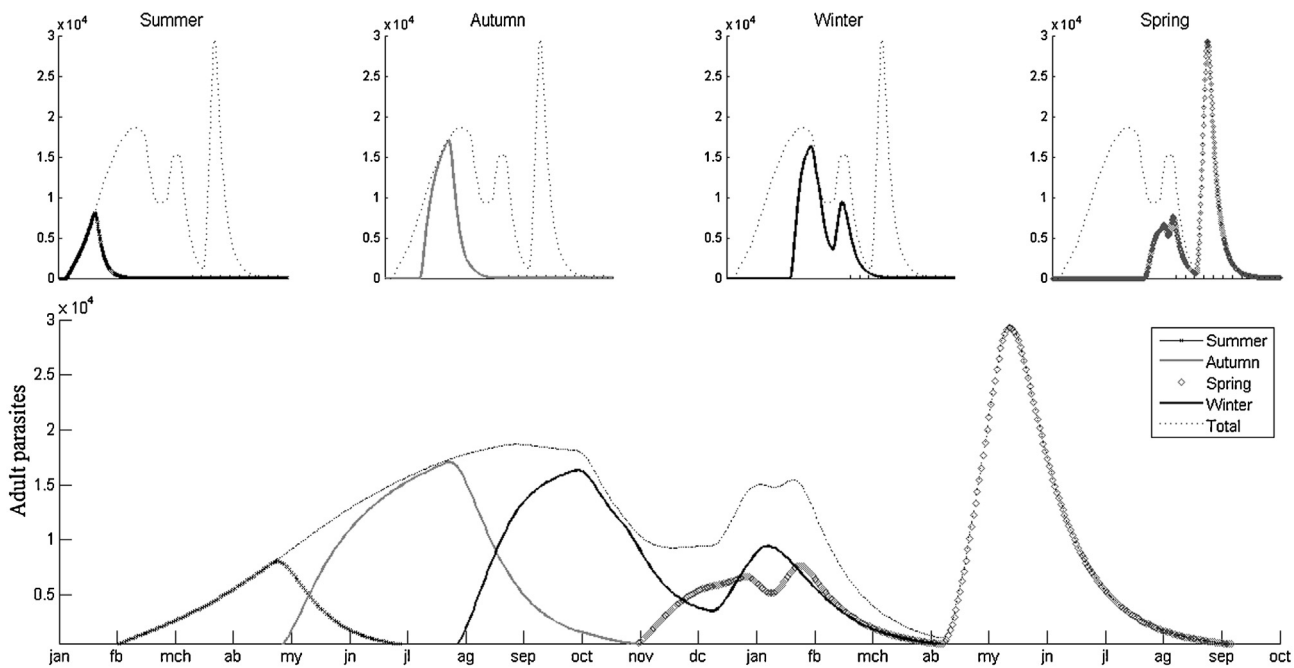


Fig. 6. Results of simulations with seasonal availability of L3 larvae in pasture. The sum of all simulations (Summer, Autumn, Winter and Spring) is called “Total” (···). It shows how the larvae produced during each season contribute to the full-year’s dynamics.

From this date on until December the population decreased and then increased to reach a new maximum in mid-January, however lower than the one reached in October. The population was extinct by the end of May. The peak was reached in mid-January is a consequence of the first and unique “wave” of disinhibition. The wave is unique because the arrested development occurred before October.

**3.1.3.3. Spring.** When the L3 larvae were ingested in Spring, the adult population survived in the host for 9 months. Most of the L3 ingested during this season arrested their development and then resumed it in two waves, one in January and the second in April. The population increased with small oscillations until it reached a maximum in February. The first wave of disinhibition is not clearly seen in the plot because it coincides with the L3 that are ingested at the same time and did not arrest their development. The second wave of disinhibition allowed the population to reach a maximum value in mid-May which is larger than that of February. This absolute maximum reached in May makes evident that most of the L3 larvae ingested in Spring arrested their development.

#### 4. Conclusions

The model proposes an original way to describe the parasitic stage of the cycle life of *O. ostertagi* combining bibliographic and empirical knowledge.

The flexibility of the model allows simulating several situations for analyzing the effect in the population dynamics of variations in temperature and photoperiod as well as the seasonal effect. From the results obtained from these simulations we can conclude that effect of hypobiosis diminishes when the photoperiod is shorter and the average temperature is lower. It is worth noting that in all cases the population showed two waves of disinhibition, one more important than other. From lower to higher latitudes (North to South in the Southern Hemisphere), the importance of the wave (abundance of parasites that reassume their development) shifted from April (second wave) to December (first wave).

If we consider that summer months in the North of Argentina have less favorable conditions for larvae (hot and dry weather) than in the South, it seems clear that the adult population will attempt

“to avoid” producing eggs during summer. In the simulations of lower latitude populations the second wave of disinhibition is more abundant than the first and occurs in autumn, when the temperature starts decreasing.

It was mentioned earlier that research carried out under laboratory conditions (Fernández et al., 1999; Fiel et al., 2009) allowed estimating that the photoperiod ranging from 12 h 11 min to 14 h 55 min induces the largest proportion of ingested L3 to arrest their development. The results obtained from the simulations are consistent with the effects of the photoperiod being observed in the study area of Tandil during the spring season. This leads us to ask whether the behavior is a matter of local parasite populations or, indeed, the range of photoperiod favorable to inhibition–disinhibition is as obtained in the laboratory. We believe it would be important to replicate this study in the field with livestock parasites in different production areas of Argentina to corroborate this hypothesis.

Analysis of the model responses to changes in the input series suggests that it may be a good tool for the generation of strategic control, when combined with the model of free-living stages developed in Chaparro et al. (2011).

### Acknowledgments

The authors wish to thank the Universidad Nacional del Centro de la Provincia de Buenos Aires (UNCPBA), and National Council for Scientific and Technological Research (CONICET) for their financial support.

### References

- Caswell, H., 2001. *Matrix Population Models*, second ed. Sinauer Associates, Inc., Sunderland, MA.
- Chaparro, M.A.E., Canziani, G.A., 2010. A discrete model for estimating the development time from egg to infecting larva of *Ostertagia ostertagi* parametrized using a fuzzy rule-based system. *Ecological Modelling* 221, 2582–2589.
- Chaparro, M.A.E., Canziani, G.A., Saumell, C.A., Fiel, C.A., 2011. Estimation of pasture infectivity according to weather conditions through a fuzzy parametrized model for the free-living stage of *Ostertagia ostertagi*. *Ecological Modelling* 222, 1820–1832.
- Couvillion, C.E., Hawkins, J.A., Evans, R.R., Belem, A.M.G., 1996. Seasonal pattern of inhibition of *Ostertagia ostertagi* in calves in northeast Mississippi. *Veterinary Parasitology* 65, 283–287.
- Descarga, C., Davies, P., Kloster, A., Rubino, D., 1994. Parasitismo gastrointestinal en terneras A Angus en la región subhúmeda sudeste de Córdoba. *Therios* 23, 620–634.
- Fernández, A.S., Fiel, C.A., Rodríguez, E.M., Fusé, L.A., Sominson, P.A., Cattoni, P.V., 1992. Parásitos internos en vaquillonas lecheras de recría. I. Efecto sobre la ganancia de peso. II. Metodología de control. III. Estudio epidemiológico. *Veterinaria Argentina* 9, 473–485.
- Fernández, A.S., Fiel, C.A., Steffan, P.E., 1999. Study on the inductive factors of hypobiosis of *Ostertagia ostertagi* in cattle. *Veterinary Parasitology* 81, 295–307.
- Fiel, C.A., Steffan, P.E., Vercesi, H.M., Ambrústolo, R.R., Catania, P., Casaro, A.P., Entrocasso, C.M., Biondani, C.A., 1988. Variación estacional del parasitismo interno de bovinos en el sudeste de la Prov de Buenos Aires (Argentina) con especial referencia al fenómeno de hipobiosis. *Revista Medicina Veterinaria (Bs. As.)* 69, 57–64.
- Fiel, C.A., Saumell, C.A., Fusé, L.A., Florez Gálvez, J., Freije, E., Iglesias, L., Steffan, P., 2009. Estudio de la dinámica de la inhibición–desinhibición de *Ostertagia ostertagi* en terneros del centro de la provincia de Buenos Aires. Resultados preliminares. *Revista Medicina Veterinaria (Bs. As.)* 90 (1/2), 4–8.
- Fiel, C.A., Fernández, A.S., Rodríguez, E.M., Fusé, L.A., Steffan, P.E., 2012. Observations on the free-living stages of cattle gastrointestinal nematodes. *Veterinary Parasitology* 187, 217–226.
- Klir, G.J., Yuan, B., 1995. *Fuzzy Sets and Fuzzy Logic: Theory and Applications*. Prentice Hall, Upper Saddle River, NJ.
- Langrová, I., Makovcová, K., Vadlejch, J., Jankovská, I., Petrtýl, M., Fechtner, J., Keil, P., Lytvynets, A., Borkovcová, M., 2008. Arrested development of sheep strongyles: onset and resumption under field conditions of Central Europe. *Parasitology Research* 103, 387–392, <http://dx.doi.org/10.1007/s00436-008-0984-6>.
- Leathwick, D.M., Vlassoff, A., Barlow, N.D., 1992. A model for nematodiasis in New Zealand lambs. *International Journal for Parasitology* 22, 789–799.
- Lützelshwab, C.M., Fiel, C.A., Pedonesse, S.I., Najle, R., Rodríguez, E., Steffan, P.E., Saumell, C., Fusé, L., Iglesias, L., 2005. Arrested development of *Ostertagia ostertagi*: effect of the exposure of infective larvae to natural spring conditions of the Humid Pampa (Argentina). *Veterinary Parasitology* 127, 253–262.
- Nguyen, H.T., Walker, E.A., 1997. *A First Course in Fuzzy Logic*. CRC Press, Boca Raton.
- Suárez, V.H., 1990. Inhibition patterns and seasonal availability of nematodes for beef cattle grazing on Argentina's western Pampas. *International Journal for Parasitology* 20, 1031–1036.
- Suárez, V.H., 2005. Evaluación de las pérdidas provocadas por las parasitosis internas. *Motivar (Bs. As.)* 3 (33), 10–11.
- Ward, C.J., 2006a. Mathematical models to assess strategies for the control of gastrointestinal roundworms in cattle 1. Construction. *Veterinary Parasitology* 138, 247–267.
- Ward, C.J., 2006b. Mathematical models to assess strategies for the control of gastrointestinal roundworms in cattle 2. Validation. *Veterinary Parasitology* 138, 268–279.